Identification of *sirm,* a Novel Insulin-regulated SH3 Binding Protein That Associates with Grb-2 and FYN*

Paola Salvatore‡§, Carla R. Hanash‡, Yoshiaki Kido‡, Yumi Imai¶, and Domenico Accili‡∥

From the ‡Developmental Endocrinology Branch, NICHHD, National Institutes of Health, Bethesda, Maryland 20892 and ¶Division of Endocrinology, University of North Carolina Medical School, Chapel Hill, North Carolina 27514

We have previously developed a mouse model of insulin-resistant diabetes by targeted inactivation of the insulin receptor gene. During studies of gene expression in livers of insulin receptor-deficient mice, we identified a novel cDNA, which we have termed *sirm* (Son of Insulin Receptor Mutant mice). *sirm* is largely, albeit not exclusively, expressed in insulin-responsive tissues. Insulin is a potent modulator of *sirm* expression, and *sirm* mRNA levels correlate with tissue sensitivity to insulin. The product of the *sirm* gene is a serine/threonine-rich protein with several proline-rich motifs and an NPNY motif, conforming to the consensus sequence recognized by the phosphotyrosine binding domains of insulin receptor substrate and Shc proteins. However, Sirm bears no extended homologies with other known proteins. Based on the sequences of the proline-rich domains, we sought to determine whether Sirm binds to the SH3 domains of FYN and Grb-2. We demonstrate here that Sirm binds to FYN and Grb-2 in 3T3-L1 adipocytes and that insulin treatment results in the dissociation of the Sirm·FYN and Sirm·Grb-2 complexes. We also show that Sirm is a substrate for the kinase activity of FYN *in vitro*. Based on the patterns of expression of *sirm*, its regulation by insulin, and the interactions with molecules in the insulin signaling pathway, we surmise that Sirm plays a role in modulating tissue sensitivity to insulin.

We have previously developed a mouse model of insulin-resistant diabetes by genetic ablation of insulin receptors. Lack of insulin receptors is rapidly lethal, leading to death from diabetic ketoacidosis within few days of birth (1, 2). We have reported that insulin treatment of liver extracts derived from insulin receptor-deficient $(ir^{-/-})$[1] mice resulted in tyrosine phosphorylation of a protein migrating as a 75-kDa species on SDS-PAGE. This protein was not detected in control $(ir^{+/+}$

mice) liver extracts. In the course of experiments designed to determine the identity of this tyrosine-phosphorylated protein, we isolated a novel cDNA. We termed the protein product of this cDNA *sirm* (Son of Insulin Receptor Mutant mice). *sirm* mRNA is most abundant in insulin-sensitive tissues, such as skeletal muscle, heart, fat, kidney, and liver, and is regulated by insulin both *in vivo* and in cultured cells. In fact, *sirm* mRNA expression correlates with insulin sensitivity so that it is increased under conditions of increased insulin sensitivity, for example during differentiation of 3T3-L1 cells and in diabetic ketoacidosis, and is decreased under conditions of desensitization to insulin, for example following prolonged exposure of cells to insulin. We have cloned a 3661-base pair *sirm* cDNA. The amino acid sequence predicted from *sirm* cDNA clones encodes a 600-amino acid polypeptide, bearing no extended homology to other known proteins. The Sirm protein is rich in serine and threonine residues and contains potential sites for tyrosine phosphorylation and for phosphorylation by proline-directed kinases, as well as proline-rich motifs. Immunoreactive Sirm localizes exclusively to the cytoplasm in skeletal muscle, whereas it is found partly associated with the membrane compartment in 3T3-L1 adipocytes. We show, using co-immunoprecipitation studies and GST binding assays, that Sirm binds to the SH3 domains of FYN and Grb-2 *in vitro* and in cultures of 3T3-L1 cells. Insulin treatment results in the dissociation of the Sirm·Grb-2 and Sirm·FYN complexes. Sirm also appears to be a substrate for phosphorylation by the FYN kinase. The engagement of Sirm in complex formation with adapter proteins and cytoplasmic tyrosine kinases, together with the distribution of Sirm to insulin-dependent tissues, and the regulation of *sirm* mRNA by insulin both *in vivo* and *in vitro* represent circumstantial evidence for the fact that Sirm plays a role in modulating tissue sensitivity to insulin.

EXPERIMENTAL PROCEDURES

Animals—Husbandry and genotyping of mice bearing a targeted *ir* allele have been described in previous publications (2–4).

Antibodies—Anti-phosphotyrosine antibody 4G10 was purchased from Upstate Biotechnology (Lake Placid, NY). Anti-insulin receptor antibodies were purchased from Oncogene Science (Cambridge, MA) and Santa Cruz Biotechnology (Santa Cruz, CA). Anti-FYN and anti-Grb-2 antibodies were purchased from Santa Cruz. Anti-Sirm antisera were raised by immunizing rabbits with keyhole limpet hemocyanin-conjugated peptides corresponding to amino acids 136–149 of the Sirm sequence. All antisera were affinity purified using peptide columns. For immunoprecipitation, antibodies were used at the concentrations recommended by the manufacturers. The immune complexes were captured on protein A-agarose beads (Life Technologies, Inc.) and washed three times in 1.0 ml of 50 mM HEPES, 150 mM NaCl, 0.1% Triton X-100 buffer and analyzed by SDS-polyacrylamide electrophoresis. The proteins were transferred to nitrocellulose filters for Western analysis. Blots were pre-blocked in 3% BSA in PBS and incubated with the anti-Sirm antibodies at a 1:1000 dilution in 0.3% BSA in PBS for 2 h at room temperature. Following a short wash in PBS containing 0.05% Tween 20 and 0.05% Triton X-100, a horseradish peroxidase-conjugated goat anti-rabbit antibody (Bio-Rad) was added at a 1:5000 dilution and

[1] The abbreviations used are: *ir*, insulin receptor; Grb-2, growth factor receptor binding protein-2; BSA, bovine serum albumin; SH3, src homology 3 domain; IGF-1, insulin-like growth factor type 1; IRS, insulin receptor substrate; GST, glutathione *S*-transferase; PBS, phosphate-buffered saline; RT-PCR, reverse transcription-polymerase chain reaction; EST, expressed sequence tags; nt, nucleotide(s).

Insulin-regulated Grb2- and FYN-binding Protein

A

UPSTREAM PRIMER:

5' ATG AGT ACA ACT ACC GCT GCT GGA 3' IGF-1Rsequence
    | ||| | | || || ||| |||
    CAA GGG ACA AGT TCC GCC GCT GGA   sirm sequence

DOWNSTREAM PRIMER:

5'CTA CAA CCG CGT CTT TCG GGC 3' IGF-1R sequence
   | ||| || || || ||
   ACT ACA CCG AGT CTA ACG AGC   sirm sequence

B

NPNY

sirm

gst-sirm (1-535)

peptide

sirm cDNA

marathon clones

cDNA clones

PCR product

in vitro translated product

* : tyrosine phosphorylation sites
‡ : proline-directed serine-phosphorylation sites
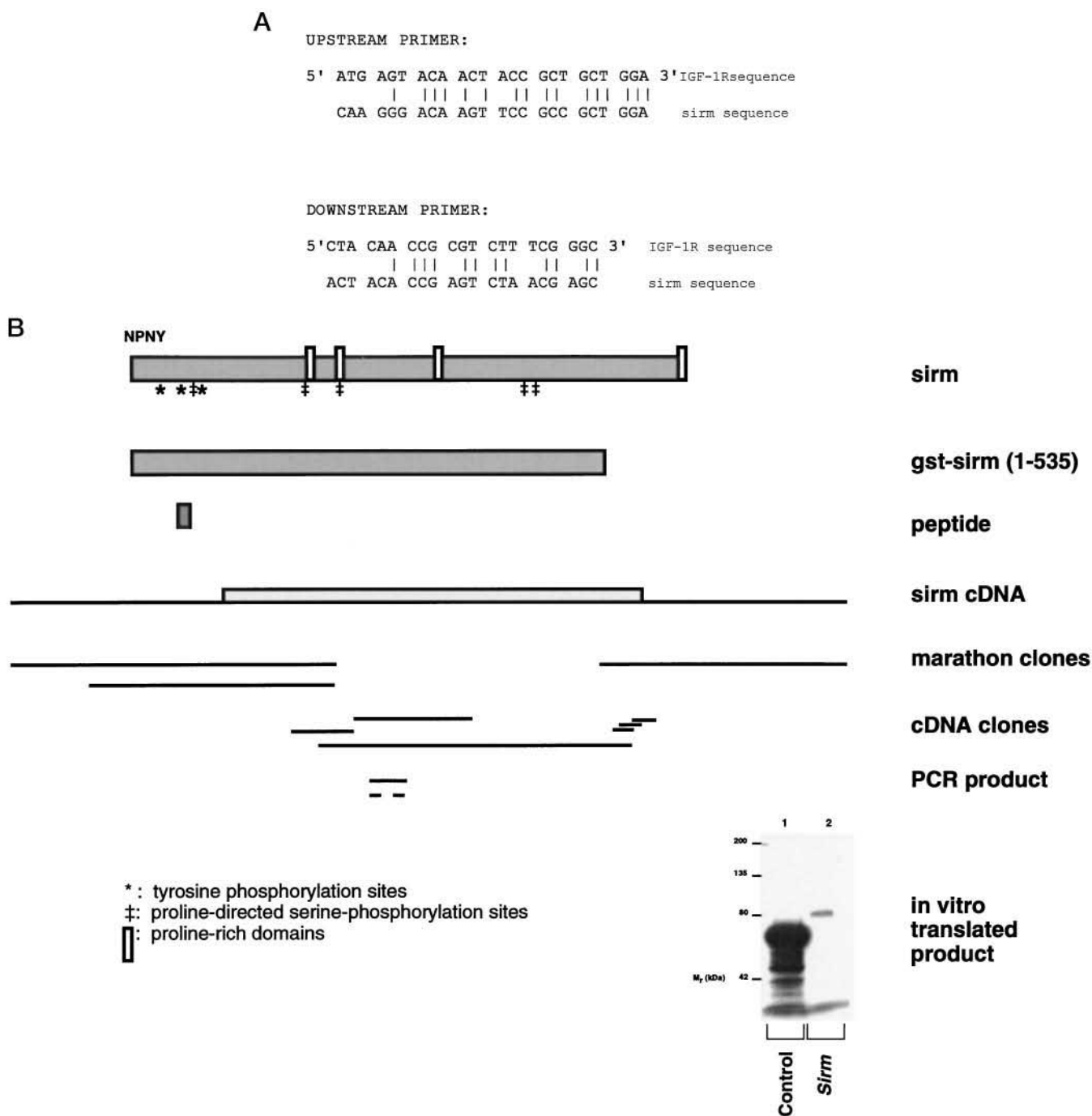▯ : proline-rich domains

Fig. 1. *A*, alignment of mouse IGF-1 receptor and *sirm* sequences. This figure shows the partial homology between the primers used to screen for IGF-1 receptor-related sequences and the *sirm* sequence. There is 66 and 57% identity between the upstream and downstream IGF-1 receptor primers and the relevant *sirm* sequences. Of note is also the virtual identity (10 out of 11 matches) at the 3′ end of the upstream primer. *B*, schematic diagram of the Sirm protein and cloning strategy. Represented from *top* to *bottom*: *, a diagram of the Sirm protein with potential tyrosine phosphorylation sites; ‡, proline-directed serine phosphorylation sites; *vertical bars*, proline-rich sequences; a diagram of the GST-Sirm used for *in vitro* phosphorylation assays; the location of the peptide used to raise antibodies; a diagram of the cDNA clone, *horizontal bar*, the sequence of which is shown in *C*, with the location of the coding sequence; the location of Marathon cDNA clones used to obtain the 5′ and 3′ end of the coding sequence; the cDNAs isolated from library screening and RT-PCR; the original *sirm* PCR product, with the primers used to identify *sirm*; and the *in vitro* translation product of the *sirm* cDNA. The sequence of the PCR primers is reported in *A*. The sequence NPNY (amino acids 34–37) is indicated above the *bar*. *C*, sequence of mouse *sirm* complementary DNA. A consensus sequence was developed using the Autoassembler software from a combination of cloned cDNA clones and amplified products from Marathon-ready cDNA. The translation start and stop codons, the putative polyadenylation signals, and some of the major structural motifs are indicated in *bold*.

incubated for 20 min. Three additional washes were performed in PBS/Tween/Triton, followed by detection of chemiluminescence using ECL (Amersham Corp.).

RNA Analysis—Total RNA was isolated from mouse livers and hind limb skeletal muscles or from SV40-transformed hepatocytes using a guanidinium isothiocyanate/acid phenol extraction procedure. Reverse transcription-PCR was performed as described previously. PCR condi-

tions were as follows: denaturation at 94 °C for 1 min, annealing at 45 °C for 1 min, and extension at 72 °C for 1 min for 30 cycles. PCR products were analyzed by gel electrophoresis. For Northern analysis, poly(A)$^+$-enriched RNA was obtained by oligo-(dT) affinity chromatography. 2–3 μg of poly(A)$^+$ RNA were size-fractionated on denaturing 1% agarose, 2.2 M formaldehyde gels and transferred to nitrocellulose membranes. The filters were probed with random-primed *sirm* cDNA. Ad-

C

```
                                                                              90
AGG TCA TGG GTG TGC CCC AGA GCA GCT TGT CTT TGN TCT GAG CCC CCT GCC CTG CCT CCC CTT TCA CCA TGT TTC CTT CGG CAA GAT TTT
                                                                              180
AAG TAC AGN AAT TCA AGA AGA TTT CTC CTA AAG NCT ATT AAT TTG AAG TGT TTT ACC TCT TGA TTG CTG GAA AAG AAT CTT AAA TTT ATT
                                                                              270
TCC AAA GTA ATT TAT AAG CAA ATN TAC TAA CAG TGG TGA GAG GAG NAC CGA CTT GAT TCC TCT ATC CTT CCA CTG TGG TCA TCT GCA TAC
                                                                              360
AGA GTC TTT CAG AGG CAA CTA GCA ATC TGG TGA GTG TGC CAT GCC AGT GGG GAG CAT TGA ATG TCC TTC ATC TCC CTC TTT CCC TAG GGA
                                                                              450
CAT TAG TCA TGA GTG CCG AGT GTG CCG GGT CAC AGA AGT GGG TCT CTC TGC ATA TGC AAA GCA CAT TTC TGG CCA ATT GCA CAA AGA TAA
                                                                              540
TGT TGA TGC CCA GGA AAG AGA AGA TGA TGG AAA GGA AGA GGA AGA GGG AGA GTT TTT TGA TAA GGA ACT TGT TCA GTT AAT ACA AGN AAA
                                                                              630
GAA AAG GCC NNA NTC GCC AAG NTG AAC CTC CCA GTG ACA GCC AAG AAG TAA ACT CAG ATG ACA GGC ACC CCC AGT GGA GAC GAG AAG CCC
                                                                              720
GAA TCC CTT ACC AAG ACA GAG AGA ATA GTC AGC CAC CAA GAC ACC ATC GTG GAC CCC CAC AGA GAG ACT GGA AAT GGG AAA AGG ATG
                                                                              810
GCT TTA ATA GTA CTA GAG GAA AAA ACA GCT TTC CAC ATT CTT TGA GGA ATA GTG GTN GAC CAA GAG GAA GTT CTG TCT GTC ATA AAG GTG CTA
                                                                              900
CAA GAG GCT CTT CAA CTT GGT TCC TTA ATC ATA GCA ATT CTG GAG GAG GNT GGC ATN CAA ACA ATG GGA TGG TAG ATT GGN ATT ATT ATG
                                                                              990
GTA CAG GAA GGA ATT CCA GTT GGC CAT TCT GAA GGA ACA GGT GGC TTT CCC AGC TGG CAC ATG AAC AAC AGT AAC GGA AAC TGG AAA TCC
                                                                 M   N   N   S   N   G   N   W   K   S
                                                                             1080
AGT GTA CGT AGT ACG AAT AGC TGG AAT TAC AAT GGC CCT GGA GAC AAA TTT CAA CAA GAC AGA AAC AGA AAT CCT AAC TAT CAA ATG GAA
S   V   R   S   T   N   S   W   N   Y   N   G   P   G   D   K   F   Q   Q   D   R   N   R   N   P   N   Y   Q   M   E
                                                                             1170
GAC ATG ACC AAG ATG TGG AAC AAG AAA TCT AAT AAG GCA ACC AAG TAC AGT GAG AGA TGC AAG TGG CAG AGG CAA GAC AGG GAC AAA
D   M   T   K   M   W   N   K   K   S   N   K   P   T   K   Y   S   Q   E   R   C   K   W   Q   R   Q   D   R   D   K
                                                                             1260
GCT GCC AAG TAC AGG AGT CCT CCT GAG GGA TAC GCA AGC GAT ACG TTT CCT TCA GAA GGC TTA CTT GAG TTC AAT TTT GAA CAG CGA GAA
A   A   K   Y   R   S   P   P   E   G   Y   A   S   D   T   F   P   S   E   G   L   L   E   F   N   F   E   Q   R   E
                                                                             1350
AGT CAA ACC ACT AAA CAA ACA GAC ACG GCA GCC TCA AAA ATT AAT GGA AAA AAT GGC ACC AAA GAC AAG TTC CGC CGC TGG ACA
S   Q   T   T   K   Q   T   D   T   A   A   S   K   I   N   G   K   N   G   T   K   A   R   D   K   F   R   R   W   T
                                                                             1440
CCT TAC CCT TCC CAG AAG ACT CTA GAT TTA CAG TCA GCC CTG AAA GAA GTC ATT GGC AGC AAG TCA GAC ACA CTA GAG AAG CCT CTC TTT
P   Y   P   S   Q   K   T   L   D   L   Q   S   A   L   K   E   V   I   G   S   K   S   D   T   L   E   K   P   L   F
                                                                             1530
AAT TTT AGC TTA ATA ACT GCA GGA CTG CGC AAA CCA GTT GAT AAA ACA AGT AAT CCT CCA GTG ATA AAA ACA CAA AAA GCA GGA CCT CCG
N   F   S   L   I   T   A   G   L   R   K   P   V   D   K   T   S   N   P   P   V   I   K   T   Q   K   A   G   P   P
                                                                             1620
GGA TCT CCA AGT CAC AAA GCC ATT TCT GAT GGC ACT GCT TTC TGT GAG GTG CCA AGA GCT TGC CCC ATT ACC GAG CAA TCT GAG CCA CAT
G   S   P   S   H   K   A   I   S   D   G   T   A   F   C   E   V   P   R   A   C   P   I   T   E   Q   S   E   P   H
                                                                             1710
CAG AAG TCA AAT AAG ATT CCA TTA CTG AAA TCC CCA CTC CTT CCA CTT CCA TCA GGT CCT CAT AAG CAA AAT TTA AAG AAC
Q   K   S   N   K   I   P   L   L   K   S   P   L   L   P   L   P   T   P   K   S   G   P   H   K   Q   N   L   K   N
                                                                             1800
CGC TCA AAG AAT AAG GAG ACA AAG TCC TTT CCT TCT GGA GAT CAC TCA CAT CTC CTG AAC ACT TCT ACT TTA GAA GGT AGC CAT GGT TCT
R   S   K   N   K   E   T   K   S   F   P   S   G   D   H   S   H   L   L   N   T   S   T   L   E   G   S   H   G   S
                                                                             1890
TCC TAC ACA TCC AAA TCA CGC GGT TTA TGT CCT CGT GTT TTA AAG GAG AAT AAA ACT GTT TCA GGC ACT CAA AAA GAA CCT GAC GAG AAG
S   Y   T   S   K   S   R   G   L   C   P   R   V   L   K   E   N   K   T   V   S   G   T   Q   K   E   P   D   E   K
                                                                             1980
TTA AAT AAC ACA TCA CAG AAA GCC CAA GAC ACA GTG CTA CAG TGT CCC AAA ACA CTG CAG AAT CCA CTC CCT ACC ACA CCC AAA AGG ATG
L   N   N   T   S   Q   K   A   Q   D   T   V   L   Q   C   P   K   T   L   Q   N   P   L   P   T   T   P   K   R   M
                                                                             2070
GAG AAC GAT GCA AAA GAA AGT AGT GTG GAA GAG TCT GCC AAA GAC TCT CTG AGC ATC GAG TCT CAG CCA CAC TCA GCT GGA AAC AGT GCC
E   N   D   A   K   E   S   S   V   E   E   S   A   K   D   S   L   S   I   E   S   Q   P   H   S   A   G   N   S   A
                                                                             2160
ATG ACA TCT GAT GCA GAA AAC CAT GGC ATA AAA AGT GAA GGT GTG GCT TCA CTG ACC ACA GAG GTT GTG TCC TGC AGC ACT CAC ACC GTG
M   T   S   D   A   E   N   H   G   I   K   S   E   G   V   A   S   L   T   T   E   V   V   S   C   S   T   H   T   V
                                                                             2250
GAT AAG GAA CAA GGG AGC CAG ATC CCA GGA ACA CCC GAG AAC CTC TCC ACC TCC CCA CGT AAT TCC ACA GTC CTC CAG AAA GAG GCT GAG
D   K   E   Q   G   S   Q   I   P   G   T   P   E   N   L   S   T   S   P   R   N   S   T   V   L   Q   K   E   A   E
                                                                             2340
GTA CAA GTG TCA GCA GCG ACC AGC CCA CAC TCT GGC TTA CTG CTA GAC TTG AAG ACC TCT CTA GAT GCG CAG GAC AAC AAC CTT GTT
V   Q   V   S   A   A   T   S   P   H   S   G   L   L   L   D   L   K   T   S   L   E   D   A   Q   D   N   N   L   V
                                                                             2430
AAA TCT GAT GGA CCT TTT GGG ACT GAG AGC TTT GGG GAC ACT AGC CTG GAT ACA GAG CTT CAA AAA CCT GAT CTC AAT AAT CAG CCC CCA
K   S   D   G   P   F   G   T   E   S   F   G   D   T   S   L   D   T   E   L   Q   K   P   D   L   N   N   Q   P   P
                                                                             2520
GGC ACG CTT CTT CCC GAA CTA AGT AAA CTT GGT TTT CCC GCC TCG CTC CAG AGA GAT CTA AGC CGA CAC ATC AGT TTG AAG TCC AAA ACA
G   T   L   L   P   E   L   S   K   L   G   F   P   A   S   L   Q   R   D   L   S   R   H   I   S   L   K   S   K   T
                                                                             2610
GGA ACA CAT CTC CCA GAG CCA AAC CTC AAT AGC GCT CGA CGA ATT CGC AAT GTT AGT GGC CAT AGA AAG AAT GAA ACA GAA AAG GAA TCT
G   T   H   L   P   E   P   N   L   N   S   A   R   R   I   R   N   V   S   G   H   R   K   N   E   T   E   K   E   S
                                                                             2700
GGG CTT AAG CCA ACC CTA CGA CAG ATT CTA AAT GCA TCA CGG AGG AAA GGT CAA CTG GGA ACA GGT CAT TCA GCA AGT AAC AAG AAA AAG
G   L   K   P   T   L   R   Q   I   L   N   A   S   R   R   K   G   Q   L   G   T   G   H   S   A   S   N   K   K   K
                                                                             2790
CAA GAG CTG GGC AAA GGC TTA CCC AGG TGT GTG CCT CTC ATA CCT GTC CTT GGA TTC TTT TAA AGG TTA CCA CAC ATT GGC CTT GAT TAA
Q   E   L   G   K   G   L   P   R   C   V   P   L   I   P   V   L   G   F   F   Ter
                                                                             2880
AAC CAA GTT CTT GTT CAA CTT AAA TTA AAC TTG TGC CAA AAA TAC CCA TTG TAG ATG TCT GCT TTA ATT CAG TAT TAA GCA CTG ACT GTT
                                                                             2970
CCT ATA TGA CAC GTG TAA TAG TCT GTC TTG GCA GAG GAT GCC ATT AAA ATG GAG GCA CCT GAG ATA CTA ATT GGA CCT AGG ATT ACA TAC
                                                                             3060
GTC ATC AGA AAT CTG TCA CTT TAG TTC AGA TGG ACT AGA ATG TGC TGT CTC TGA ATC TTA ATG TTT GGA ACC AAT GGT AAA AAT TTT TGA
                                                                             3150
TTT GTT TGC TTG CTT GCT TTT TGG TTT TCA AGA TGG GGT TTC TCT ATA TAG CCC TGT CTG GTC TAT AGA ACA GAC TGG CCT CGA ACT AAG
                                                                             3240
AGA AGG CCT GCT TTT GCC TGA GAT TAA AGG CAT GTN CCA CCA CCG CCC TGC TAG TGG TCA ATT TTT TCA ACT ACC TGT TGT TAC TAC CTT
                                                                             3330
TCA CTG AGC TTG TGG AAT CCC CCA TAG GCA TTC TGG GTA CTA CAG AGA GGA CTG CAG AAT GCT TTC TCT TAA GCT CAC TCA GAG CAT GAG
                                                                             3420
CTT GTG GAA NCC CCC ATA GNC ATT CTG GGT ACC TAC AGA GAG GNC TNC AGA ATG CTT TCC TCT TAA GCT CAC CTC AGA NCA TCC TTG AGT
                                                                             3510
TGC TGT TCT AAG TGG TCA AGA AGT GCT CAG CAT AGG NTC CAA CTT GGA AAA TCA TAG TTT TGC AAC GAT GTA AGT GTA GCC CTC CAG GCT
                                                                             3600
CAG GGA CTT TAC TGT TGT TGG TTC ATT TGC CTT GTT TTC CTT TCT TAG TCC TTT TCC AAA GTT ATG GTT TGG TAA AGC AGA AAG CTT AGA

GAC CTG CTT AAT GGT TGT GAG TAC TTG GTA AGC TGG TTT CTT TGC TTT NAG AAT GTT TAC
```

Fɪɢ. 1—*continued*

ditionally, a mouse multiple tissue, an embryonic Northern blot, as well as a zoo blot (CLONTECH, Palo Alto, CA) were used to confirm the identity of the various clones isolated, to study the distribution of the *sirm* transcripts, and to analyze the presence of *sirm* gene homologues in other species. Hybridization was performed according to standard procedures.

Cloning of Full-length Sirm cDNA—Initially, a random primed *sirm* fragment obtained by RT-PCR amplification of $ir^{-/-}$ liver RNA was used to probe 10^6 plaques of mouse embryo and mouse fetal heart cDNA libraries (CLONTECH). Hybridization and plaque purification of individual positive clones were carried out according to standard methods. However, only partial cDNA clones could be isolated from these librar-

ies. To isolate full-length clones, mouse heart Marathon-ready cDNA (CLONTECH) was amplified using primers derived from the 5′ and 3′ end of the available sequence. Amplification was carried out as suggested by the manufacturer, with a mixture of Klenow and *Taq* polymerase. Amplified products were subcloned into a PCR II vector (Invitrogen, Carlsbad, CA) and sequenced using cycle sequencing with fluorescent dideoxy terminators (Applied Biosystems, Foster City, CA) on 373 and 377 Applied Biosystems sequencers. Each partial clone was hybridized with multiple tissue Northern blots as well as Northern blots of $ir^{-/-}$ mice to confirm that amplified sequences derived from the same original transcripts. Multiple subcloned fragments were analyzed to confirm the nucleotide sequence. Sequence alignment was carried out

A

class I consensus	+ P Ψ P P Ψ P
class II consensus	Ψ P P Ψ P P +

B

src sh3 cons				R	P	L	P	X	Ψ	P
fyn cons				R	P	L	P	P	L	P
grb2 cons	+	Θ	D	X	P	L	P	X	L	P
sirm (plus or) 328	T	L	Q	N	P	L	P	T	T	P 337
sirm (minus or) 240	S	K	P	T	P	L	P	L	L	P 231
consensus					P	L	P		L	P

C

SIRM 224			K	I	P	L	L	K	S	P	L	L	P	L	P	T	P	K S G P H K Q 246
CR 16 279			L	A	P	Y G Y	P	P	L	L	P	L	P	P	I	P P L H L 259
SH3 BP-2 231					P	-	-	-	S	P	L	L	P	P	P	P	K R G L P D 246
ras-GAP SH3 185	I	E	E	P	L	E	E	S	S	H	E	P	E	P	E S E 203
abi-2 112	P V R P	P	V	V	P N D Y	V P	S	P	T R N M A P 132
consensus					P	:			S	P	L	L	P		P		P	

FIG. 2. **Alignments of Sirm proline-rich domains with consensus motifs that bind the SH3 domains of FYN and Grb2.** *A*, consensus sequences for class I and class II SH3 binding; *B*, alignment of two potential SH3 binding domains (amino acids 231–240 and 332–337) in the Sirm sequence with the consensus Src, FYN, and Grb2 SH3 binding sites. *C*, alignment of the proline-rich domain encoded by amino acids 231–240 of Sirm with the SH3 binding domains of CR16 (15), SH3 BP-2 (16), Ras GAP-SH3 (17), and Abi-2 (18).
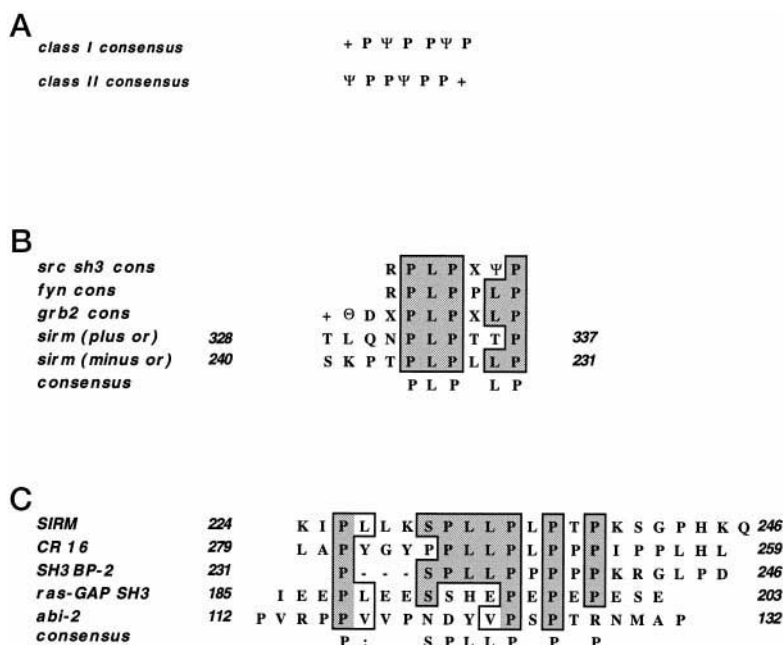
using the Autoassembler software (Applied Biosystems) to develop a consensus sequence. Ambiguities were further resolved by visual inspection of electropherograms.

Expression of GST-sirm Fusion Products—An 1800-nt fragment of the mouse *sirm* cDNA was amplified from Marathon-ready mouse heart cDNA. The upstream primer 5′ GAA TTC TCC AGC TGG CAC **ATG** AAC AAC AGT3′ (nt 949–972) contained an additional *Eco*RI site in frame with the ATG initiation codon (bold face). The downstream primer spanned nt 2924–2901. The amplified product was digested with *Eco*RI to generate a 1590-nt fragment, which was subsequently subcloned into the *Eco*RI site of pGEX2T (Pharmacia Biotech Inc.). The amplified fragment was entirely sequenced to rule out nucleotide substitutions during the amplification procedure. Bacterial cultures were obtained as indicated by the manufacturer, and the recombinant GST-Sirm fusion protein was isolated by affinity chromatography using glutathione-Sepharose beads.

Tissue Isolation—Whole E13.5 and 18.5 mouse embryos, or livers, hind limb muscles, hearts, epididymal fat pads, and kidneys derived from adult mice were finely minced and homogenized using a glass-glass pestle in 1 mM NaHCO$_3$ containing a mixture of protease inhibitors (Boehringer Mannheim). 20 μg of whole tissue extracts were prepared for SDS-gel electrophoresis as described (2).

Subcellular Fractionation—In some experiments, subcellular fractions were obtained from cultures of 3T3-L1 cells or from mouse skeletal muscle. After resuspending the cells or tissue in 1 mM NaHCO$_3$ buffer as described above, nuclei were removed by a low speed centrifugation (1000 × *g*) for 10 min, followed by high speed centrifugation (20,000 × *g*) to pellet the microsomal fraction and separate the cytosol. The crude microsomal homogenate was solubilized in 50 mM HEPES (pH 7.6) 150 mM NaCl containing 1% Triton X-100 and protease inhibitors, followed by centrifugation at 100,000 × *g* to remove the insoluble material.

Insulin Stimulation of 3T3-L1 Cells and SV40-transformed Hepatocytes—3T3-L1 cells were differentiated as described (5). Cultures of differentiated 3T3-L1 cells or confluent SV40-transformed hepatocytes derived from *ir*$^{-/-}$ mice or from *ir*$^{+/+}$ mice were grown in 100-mm Petri dishes as described. Following incubation overnight in 1% dialyzed fetal bovine serum (3T3-L1) or for 4 h in 1% insulin-free BSA (SV40-transformed hepatocytes), cells were incubated in the presence or absence of 100 nM insulin for various lengths of time at 37 °C. Thereafter, cells were frozen in liquid N$_2$ and thawed in solubilization buffer (1% Triton X-100 in 50 mM HEPES, 150 mM NaCl, 100 mM NaF, 4 mM sodium orthovanadate, 1 mM EDTA, 4 mM sodium pyrophosphate). For RNA analysis studies, SV40-transformed hepatocytes were incubated with insulin (1 or 100 nM) for 4 h, frozen in liquid N$_2$, and thawed for RNA extraction as outlined above.

In vitro transcription/translation was performed using a coupled rabbit reticulocyte system (Promega, Madison WI) according to the manufacturer's instructions.

GST Fusion Protein Binding Assay—The GST fusion proteins used in these studies are as follows: mouse c-Abl type IV SH3 domain (amino
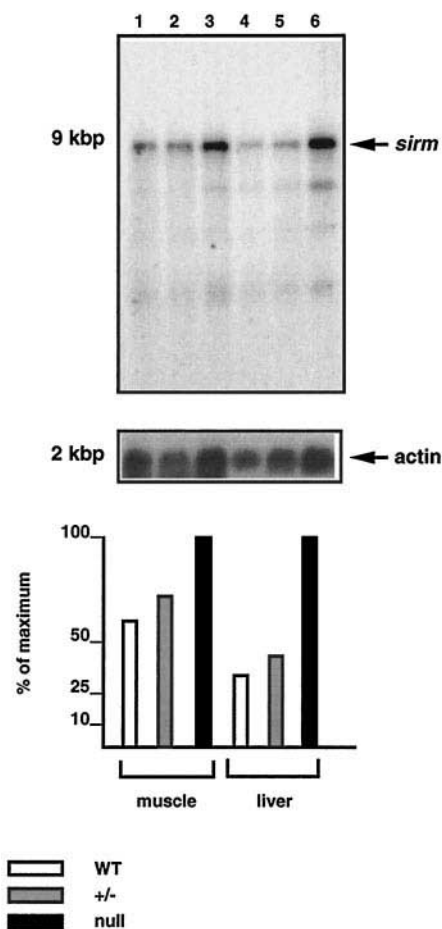
FIG. 3. **Sirm mRNA levels are increased in mice lacking insulin receptors.** RNAs were isolated from newborn mouse muscle (*lanes 1–3*) and liver (*lanes 4–6*). The blot was hybridized with a *sirm* cDNA and reprobed with an actin probe to normalize for RNA content. Scanning densitometry was employed to quantitate levels of *sirm* mRNA. Quantitative representation of the data is presented at the *bottom* of the figure. In each set of tissues, the highest levels of *sirm* mRNA were normalized to 100%. For each lane, RNAs from 3 to 5 animals were pooled. 2 μg of poly(A)$^+$ were applied to *lanes 1–3*, whereas 3 μg of poly(A)$^+$ were applied to *lanes 4–6*.

acids 84–138) (6), the mouse phosphatidylinositol 3-kinase p85 SH3 domain (amino acids 1–80) (7), the human FYN SH3 domain (amino acids 84–148) (8), and the full-length mouse Grb2 (Upstate Biotechnology). Confluent monolayers of SV40-transformed hepatocytes (in two 175-cm² flasks) were solubilized in 5 ml of 1% Triton buffer. 5 μg of recombinant GST fusion protein in 0.05 ml were added to the extracts and allowed to bind for 1 h at 4 °C on a rotating wheel. Thereafter, the

material was pelleted by centrifugation and washed in 10 ml of 0.1% Triton buffer four times. The final pellet was prepared for electrophoresis as described above.

In Vitro Kinase Activity—2 units of purified FYN kinase (Upstate Biotechnology) were incubated with 1 unit of denatured rabbit muscle enolase (Sigma) in the presence of GST, or GST-Sirm, or with various concentrations of peptides corresponding to Sirm amino acid sequences 224–246 (peptide 1), 331–339 (peptide 2), and 29–40 (peptide 3). Thereafter, a phosphorylation buffer containing 50 mM HEPES (pH 7.4), 5 mM MgCl, and 10 μCi of [γ-³²P]ATP (3000 Ci/mmol, NEN Life Science Products) was added, and the reaction was incubated at room temperature for 30 min. The reaction was stopped by adding Laemmli sample buffer, and the products were analyzed by SDS-PAGE followed by autoradiography. One of two experiments is shown.

RESULTS

Cloning of Sirm—We had previously shown that insulin stimulation of liver extracts derived from $ir^{-/-}$ mice results in tyrosine phosphorylation of a protein of apparent mass of ~75 kDa that is not observed in $ir^{+/+}$ mice (see Fig. 3*B* in Ref. 2). We questioned whether this protein may share sequence similarity with the insulin receptor or its substrates. To this end, we carried out RT-PCR amplification from $ir^{-/-}$ and $ir^{+/+}$ mice liver RNA using several sets of primers, the sequences of which were derived from mouse insulin and IGF-1 receptors, as well as insulin receptor substrate-1 (IRS-1). A set of primers designed to amplify the extracellular domain of the IGF-1 receptor consistently gave rise to an additional band of slightly larger size than predicted (Fig. 1*A*). This band was unique to $ir^{-/-}$ liver RNA and was never observed in amplification experiments with $ir^{+/+}$ mouse liver RNA (data not shown). The band was isolated, sequenced, and used as a hybridization probe to isolate clones containing the *sirm* coding sequence. By using a combination of cDNA library screening and cDNA amplification techniques, we cloned a 3661-nt cDNA, with an open reading frame of 1800 nucleotides, predicted to encode a 600-amino acid polypeptide. The 5′ end of the cDNA was isolated from mouse heart Marathon cDNA (CLONTECH). Two different clones were isolated, possibly as the result of two different transcription start sites. The longest cDNA contains 962 nt of 5′-untranslated sequence; the shorter one contains 620 nt. Two non-canonical ATTAAA polyadenylation signals are found 24 and 160 nt downstream of a putative ochre termination codon. *In vitro* translation of a full-length *sirm* cDNA clone in a rabbit reticulocyte lysate yielded a peptide of 81 kDa (Fig. 1*B*).

The predicted amino acid sequence of Sirm (Fig. 1*C*) bears weak homology (20% identity in a 511-amino acid overlap) to the KSP region of the *unc*-89 gene product in *Caenorhabditis elegans* (9) and
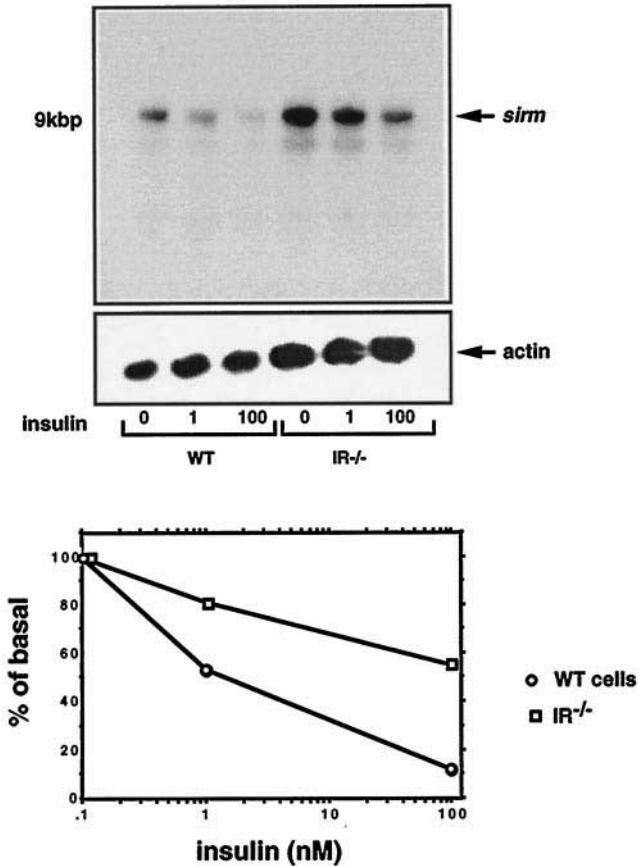
FIG. 4. **Insulin treatment decreases steady-state *sirm* mRNA levels.** Confluent monolayers of SV40-transformed murine hepatocytes derived from $ir^{+/+}$ (*lanes 1–3*) or $ir^{-/-}$ mice (*lanes 4–6*) were incubated in the presence of the indicated concentrations of insulin for 4 h. Thereafter, RNA was extracted and analyzed by Northern blot. The *upper panel* shows the result of hybridization with a *sirm* cDNA probe, whereas the *middle panel* shows the control hybridization with an actin probe. A densitometric analysis of the intensity of the bands, corrected for actin RNA, is plotted in the *bottom panel*. *Sirm* mRNA levels in untreated cells are normalized to 100%.

FIG. 5. **Tissue survey of *sirm* mRNA expression.** Mouse multiple tissue and embryonic Northern blots (CLONTECH) and a blot containing RNA derived from undifferentiated and differentiated 3T3-L1 cells were hybridized with a *sirm* cDNA as indicated in Fig. 2, *A* and *B*. The panel on the *bottom right side* shows the result of a control hybridization with actin of the 3T3-L1 blot, to demonstrate the presence of RNA from undifferentiated cells.
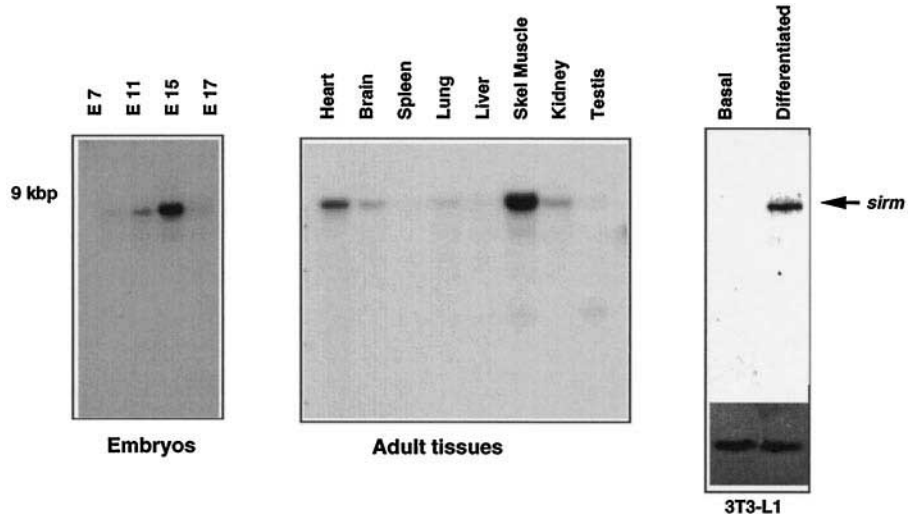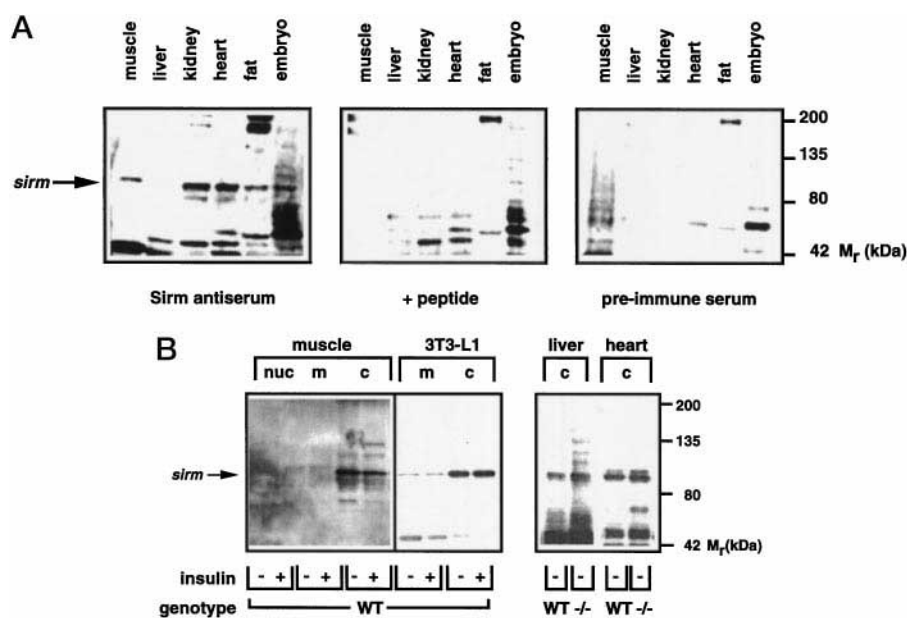
FIG. 6. *A*, tissue distribution of immunoreactive Sirm protein. Different mouse tissues, indicated on the *top*, were solubilized in NaHCO₃ buffer containing protease inhibitors. 15 μg of proteins were applied to the lanes containing muscle, heart, fat, and embryo extracts; 40 μg were applied to the lanes containing liver and kidney extracts. Proteins were separated by SDS-PAGE and transferred to nitrocellulose filters. The filters were incubated with anti-Sirm antibody (*left panel*) in the absence or presence of 1 μM competing peptide (*middle panel*). Preimmune serum was also used as control and is shown in the *right-hand panel*. *B*, subcellular localization of Sirm. Tissue extracts of mouse skeletal muscle and 3T3-L1 adipocytes were fractionated into a cytosolic and a membrane-enriched fraction (see "Experimental Procedures"). As a control, nuclei (*nuc*) were collected by low speed centrifugation during the preparation of muscle extracts and are shown in the *1st two lanes* on the *left*. The amounts of protein extracts applied were the following: 15 μg of muscle nuclei, 15 μg of muscle and 3T3-L1 membrane (*m*) and cytosol (*c*), 40 μg of liver cytosol ($ir^{+/+}$ mice), 80 μg of liver cytosol ($ir^{-/-}$ mice), 10 μg of heart cytosol ($ir^{+/+}$ mice), and 16 μg of heart cytosol ($ir^{-/-}$ mice). Proteins from each fraction were analyzed by SDS-PAGE followed by immunoblotting with anti-Sirm antibody. *WT*, wild-type
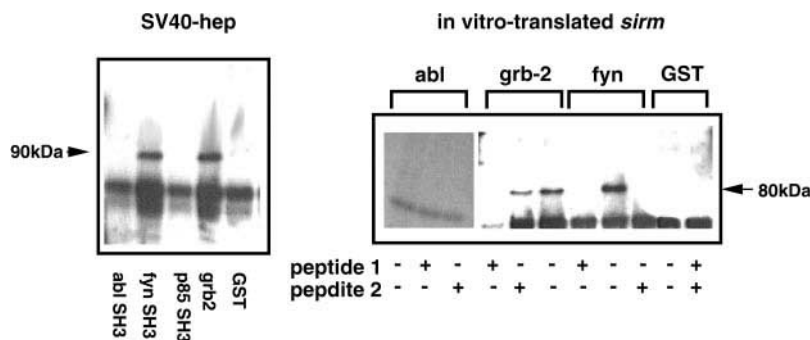
FIG. 7. **Association of Sirm with Grb2 and with SH3 domains of p85α, Abl, and FYN.** *Left panel,* GST fusion proteins encoding the SH3 domains of Abl, FYN, p85, the entire Grb2 coding sequence, or wild-type GST (5 μg) were incubated with Triton extracts of SV40-transformed murine hepatocytes (*SV40-hep*). The resulting pellets were immunoblotted with an anti-Sirm antibody. *Right panel, in vitro* translated Sirm protein (as shown in Fig. 1*B*) was incubated with the same amount of Abl, Grb2, FYN, and wild-type GST fusion protein as shown in the *left panel*, in the absence or presence of 1 μM competing peptide. The peptide sequences are as follows: *peptide 1,* IPLLKSPLLPLPTPKS; *peptide 2,* NPLPTTPKR.

to the open reading frame K08E7.5 on chromosome IV of *C. elegans* (21% identity in a 598-amino acid overlap) (10). The KSP region of the *unc*-89 gene is serine- and threonine-rich and is thought to represent a potential target for phosphorylation by cell cycle-dependent kinases. We did not detect any homology to known mammalian proteins. However, analysis of the data base of expressed sequence tags revealed that *sirm* is virtually identical to two human ESTs. The first EST corresponds to a skeletal muscle cDNA (Z19503/HSB35G062); the second one to a beta cell library cDNA (T10445) (11).

The longest *sirm* open reading frame is predicted to encode a polypeptide of 69,000 Da (Fig. 1*C*). Hydropathy profile analysis indicates that Sirm lacks a hydrophobic sequence long enough to serve as a transmembrane domain. The sequence is enriched in serines and threonines (20% of all amino acids) and in basic residues (17% arginines, lysines, and histidines). There are five potential —SP— phosphorylation sites by proline-directed ser-

ine kinases at amino acid residues 76, 189, 231, 418, and 438. Three potential sites of tyrosine phosphorylation are present at positions 37, 56, and 81. Tyr[37] is of interest in that it conforms to an NP*X*pY motif found in receptor tyrosine kinases and is thought to serve as a binding site for the phosphotyrosine binding domains of IRS and Shc molecules upon phosphorylation (12). Another interesting feature of Sirm is the presence of four proline-rich motifs, conforming to the SH3 binding consensus P*XX*P (13). Of these, sequences NPLPTTPKR (amino acids 328–336) and PLPLLPSK (amino acids 240 to 233, in reverse orientation) share homology with the Src and Grb2 SH3 consensus binding site RPLPPLP (14) (Fig. 2*B*). The sequence between amino acids 224 and 246 conforms to a consensus PΨ*XX*SPLLP*X*P*X*P sequence, where Ψ indicates a hydrophobic amino acid, found in the following four known SH3 domain-binding proteins: CR16, a protein encoded by a brain-specific mRNA regulated by glucocorticoids (15); SH3 BP2, a protein

Fig. 8. **Sirm binds to FYN and Grb-2 in 3T3-L1 cells.** Detergent extracts of undifferentiated or differentiated 3T3-L1 cells were incubated with various antibodies, as indicated on the *top* of each panel. Thereafter, the immune complexes were centrifuged for 5 min at 14,000 rpm and washed as described under "Experimental Procedures." The samples were prepared for electrophoresis and analyzed by immunoblotting with an anti-Sirm antibody.
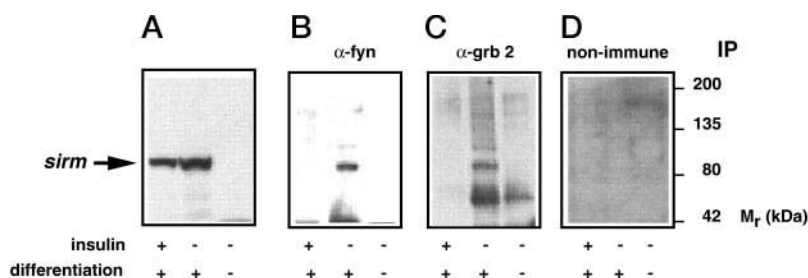
that binds to the Src, Nck, Grb-2, and Abl SH3 domains (16); the Ras-GAP SH3 binding protein (17); and Abi-2, a protein cloned based on its ability to bind with high affinity to the SH3 domain of Abl (18). It should be noted, however, that the proline-rich domains of SH3 BP-2 and Abi-2 that are homologous to Sirm are not the same as those implicated in Abl binding (16, 18).

sirm mRNA Is Overexpressed in Liver and Skeletal Muscle of Mice Lacking Insulin Receptors—*sirm* was originally detected in RNA derived from $ir^{-/-}$ mice. Next, we asked whether failure to detect *sirm* in the same assay in $ir^{+/+}$ mice could be due to overexpression of *sirm* in $ir^{-/-}$ mice compared with normal littermates. Northern blotting analysis was performed on pooled RNAs derived from skeletal muscle and liver of three to five $ir^{+/+}$, $ir^{+/-}$, and $ir^{-/-}$ mice (Fig. 3). In liver of $ir^{-/-}$ mice, *sirm* mRNA levels were 3-fold higher than in $ir^{+/+}$ mice (Fig. 3, *lanes 4* and *6*) after correcting for the amount of actin mRNA (*lower panel*), whereas in skeletal muscle they were 40% higher (*lanes 1* and *3*). Intermediate variations were observed in $ir^{+/-}$ mice (*lanes 2* and *4*).

Expression of Sirm Correlates with Tissue Sensitivity to Insulin—To determine further whether expression of *sirm* is under regulation by insulin, we studied the effect of insulin on *sirm* expression in SV40-transformed hepatocytes derived from $ir^{-/-}$ and $ir^{+/+}$ mice. Cells derived from $ir^{-/-}$ mice are devoid of insulin receptors but possess about 50,000 IGF-1 receptors/cell.[2] After treatment with insulin (1 or 100 nM), RNA was isolated and analyzed by Northern blotting with a ^{32}P-labeled *sirm* cDNA (Fig. 4). 4 h treatment of normal cells with 1 nM insulin led to a 50% decrease of *sirm* expression, and 100 nM insulin led to a 90% decrease (Fig. 4, *lanes 1–3*). In contrast, in $ir^{-/-}$ cells, 1 nM insulin decreased *sirm* mRNA levels by 20% and 100 nM insulin by 45% (Fig. 4, *lanes 4–6*). Thus, expression of the *sirm* gene is decreased following prolonged exposure of cells to insulin. The ID_{50} for insulin inhibition of *sirm* expression is ~1 nM in $ir^{+/+}$ cells and ~100 nM in $ir^{-/-}$ cells. This observation suggests that insulin regulates *sirm* expression in $ir^{-/-}$ cells by binding to IGF-1 receptors. In fact, insulin would be predicted to bind to IGF-1 receptors with about 100-fold lower affinity compared with insulin receptors.

Sirm Is Prevalently Expressed in Insulin-responsive Tissues—We performed a tissue survey of *sirm* gene expression (Fig. 5). During mouse embryonic development, *sirm* expression peaks in mid-late gestation (E11–15), to then decline prior to birth (*left panel*). In adult mouse, *sirm* is most abundant in skeletal muscle and heart (Fig. 5, *middle panel*). Additionally, *sirm* is expressed in kidney, brain, and lung. Although not clearly visible on this exposure of the blot, *sirm* mRNA can be detected in liver, as demonstrated in Figs. 3 and 4. Expression of *sirm* is associated with adipocyte differentiation of 3T3-L1 cells (Fig. 5, *right panel*). Furthermore, *sirm* is identical to EST T10445, which was isolated from a pancreatic islet library (11, 19). Thus, *sirm* is expressed in virtually all insulin-responsive tissues and, at lower levels, in other organs. Similar expression

patterns were detected using Northern analysis of human RNAs (data not shown). A zoo blot (CLONTECH) was hybridized to a ^{32}P-labeled mouse *sirm* cDNA. Results indicate that homologues of the mouse *sirm* gene are present in human, rat, and yeast (data not shown).

Subcellular Distribution of Sirm and Quantification of the Protein Product in Mice—We raised a polyclonal antiserum against the peptide sequence corresponding to amino acids 136–149 of Sirm. The antiserum detected an immunoreactive species of ~90 kDa in several mouse tissues, which is specifically competed by the peptide used for affinity purification of the antiserum (Fig. 6A, compare *left* and *middle panel*). The same band is not present when preimmune serum is used for immunoblotting (Fig. 6A, *right panel*). The tissue distribution of immunoreactive Sirm protein correlates well with patterns of mRNA expression.

We next examined the subcellular localization of Sirm (Fig. 6B). Extracts of skeletal muscle and 3T3-L1 adipocytes were separated into cytosolic and membrane-enriched fractions. In skeletal muscle, immunoreactive Sirm was detected exclusively in the cytosolic fraction. In contrast, in 3T3-L1 adipocytes, a fraction of Sirm immunoreactivity corresponding to about 25% of the total was membrane-associated (Fig. 6B). Short term (5 min) stimulation with 100 nM insulin did not affect the subcellular distribution of Sirm (Fig. 6B, compare *−insulin* and *+insulin lanes*).

We also compared the levels of Sirm immunoreactivity in livers and hearts of $ir^{+/+}$ and $ir^{-/-}$ mice (Fig. 6B, compare *WT* and *−/− lanes*), but we failed to detect the difference predicted on the basis of the Northern blot shown in Fig. 3. It is possible that the discrepancy between levels of mRNA and immunoreactivity is due to impaired recovery of immunoreactive Sirm protein in insulin receptor-deficient mice caused by their advanced metabolic derangement.

Sirm Binds to Grb-2 and to the SH3 Domain of FYN in Vitro—The amino acid sequence of Sirm contains four proline-rich domains that could potentially serve as binding sites for SH3-containing proteins. Based on the homology between these domains and the known binding specificities of Grb-2 and FYN (Fig. 2B), we investigated whether Sirm could bind to Grb-2 or FYN SH3-GST fusion proteins *in vitro*. Furthermore, in view of the consensus sequence among Sirm (amino acids 224–246) and several Abl-binding proteins, we also included the Abl SH3-GST protein in these experiments, as well as the p85α SH3-GST as a negative control. GST fusion proteins containing the SH3 domains of the p85α subunit of phosphatidylinositol 3-kinase (7), Abl (6), FYN (8), and full-length Grb-2 were expressed in *Escherichia coli*, purified, and incubated with detergent extracts of SV40-transformed hepatocytes. Immunoblotting of the resulting gels with the Sirm antibody showed that Sirm binds to GST-Grb2 and GST-FYN SH3 but not to the SH3 domains of p85α or Abl (Fig. 7, *left panel*). To characterize better the nature of this interaction, we incubated *in vitro* translated Sirm with GST fusion proteins in the absence or presence of two proline-rich peptides derived from the Sirm sequence (Fig. 7, *right panel*). Sirm binding to Grb-2 was

[2] K. Rother, Y. Imai, and D. Accili, manuscript in preparation.
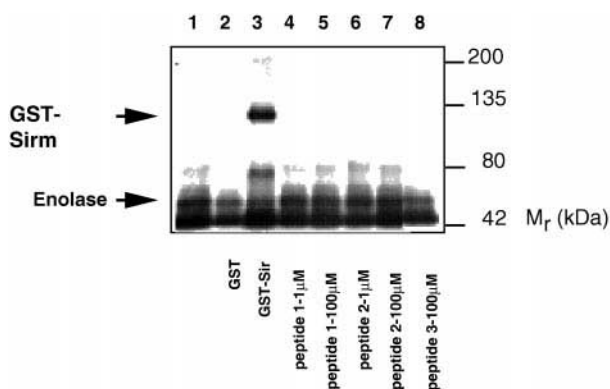
FIG. 9. **Sirm is a substrate for the *in vitro* kinase activity of FYN.** Purified FYN kinase was incubated with denatured enolase (*lane 1*) and GST (*lane 2*) or GST-*sirm* (*lane 3*), or with various concentrations of proline-rich peptides 1 (corresponding to the sequence 224–246), 2 (corresponding to the sequence 331–339), and with a control peptide (corresponding to the sequence 29–40). Thereafter, a phosphorylation mixture containing MgCl and [γ-^{32}P]ATP was added, and the reaction was incubated at room temperature for 30 min. The reaction products were analyzed by SDS-PAGE followed by autoradiography. One of two experiments is shown.

inhibited by incubating extracts in the presence of the proline-rich peptide IPLLKSPLLPLPTPKS (*peptide 1*, Fig. 7) but not by peptide NPLPTTPKR (*peptide 2* Fig. 7), whereas binding to FYN SH3 was inhibited by both peptides, indicating that, at least in this reconstitution experiment, Sirm can interact with Grb-2 and FYN directly, through one (Grb-2) or more (FYN) proline-rich sequences (Fig. 2).

Sirm Binds to Grb-2 and FYN in 3T3-L1 Cells—Insulin treatment dissociates the sirm·Grb-2 and sirm·FYN complexes. Next, Sirm binding to SH3 domain proteins was investigated in cultures of 3T3-L1 cells. We questioned whether the association between Sirm and Grb-2 or FYN could be detected *in vivo* by way of co-immunoprecipitation assays (Fig. 8). As shown in *A*, Sirm expression is greatly increased following differentiation of 3T3-L1 cells and is decreased by ~30% by treatment with 100 nM insulin for 30 min. Following immunoprecipitations with the various antibodies, proteins bound to the immune complexes were analyzed by SDS-PAGE and immunoblotting with anti-Sirm antibody. Following immunoprecipitation with FYN antibody (Fig. 8*B*), immunoreactive Sirm could be detected in differentiated 3T3-L1 cells under basal conditions. However, insulin treatment resulted in the complete disappearance of FYN-bound Sirm, indicating that FYN is indeed complexed with Sirm in 3T3-L1 cells and that insulin treatment causes dissociation of the Sirm·FYN complexes. Likewise, Sirm could be detected in Grb-2 immunoprecipitates under basal conditions but not following insulin treatment (Fig. 8*C*). No Sirm immunoreactivity is present following immunoprecipitation with nonimmune serum (Fig. 8*D*). Control immunoblotting experiments with Grb-2 and FYN antibodies indicate that the same amount of protein is present in all lanes (not shown).

Sirm Is a Substrate for the Kinase Activity of FYN in Vitro, the Failure of Sirm to Modulate FYN Kinase—The activity of Src family kinases, such as FYN, is regulated through interactions of cellular proteins with their SH2 and SH3 domains. For example, deletion of either domain leads to constitutive activation of the Abl or Src kinases (20–22). We wanted to determine whether Sirm could modulate FYN kinase activity through SH3 domain interactions. GST-Sirm (amino acids 1–535) was incubated with partially purified FYN and [γ-^{32}P]ATP (Fig. 9), and the kinase activity of FYN was measured using enolase as a substrate in the presence or absence of various concentrations of the two proline-rich peptides that interact with FYN (Fig. 9, *lanes 4–9*). Neither GST-Sirm (amino acids 1–535) nor

Sirm-derived peptides altered phosphorylation of enolase by FYN. Furthermore, FYN catalyzed the phosphorylation of GST-Sirm (*lane 3*). We have also shown that Sirm can serve as a substrate for the insulin and IGF-1 receptor tyrosine kinases *in vitro* (not shown).

DISCUSSION

In this paper, we report the identification and a preliminary characterization of a novel gene, which we have termed *sirm*. Even though the identification of *sirm* was the serendipitous by-product of a search to identify proteins uniquely expressed by insulin receptor-deficient mice, several features of the *sirm* gene prompted us to investigate it further. First, insulin is a potent regulator of *sirm* mRNA expression, so that *sirm* mRNA is up-regulated in conditions of increased tissue sensitivity to insulin, such as differentiation of 3T3-L1 cells and diabetic ketoacidosis, whereas it is down-regulated by prolonged insulin treatment. Interestingly, the highest levels of *sirm* expression are found in insulin-sensitive tissues, such as skeletal muscle, heart, fat, kidney, and liver. Indirect evidence indicates that *sirm* is also expressed in pancreatic beta cells, since an EST with virtual sequence identity to *sirm* was detected in a beta cell library (11). Interestingly, we have localized the human homologue of *sirm* to chromosome 15q15, in the genetic interval between D15S118 and D15S123, which corresponds to 32–45 centimorgans on the physical map of chromosome 15.[3] This region contains marker D15S102. In studies of Mexican American sibling pairs with non-insulin-dependent diabetes mellitus, Hanis *et al.* (23) reported a significant departure from the expected frequency of allele sharing at this marker. Further studies will be necessary to determine whether this region contains a diabetes-susceptibility locus; however, the co-localization of *SIRM* to this region is intriguing.

The sequence of Sirm contains a number of interesting features that suggest clues as to its function. In this paper, we have shown that Sirm can interact with proteins containing SH3 domains through its proline-rich motifs. In 3T3-L1 cells, Sirm associates with the Src family tyrosine kinase FYN. Binding of Sirm to FYN was predicted on the basis of a consensus binding site for the FYN SH3 domain (Fig. 2*B*) (14, 24). Interestingly, insulin treatment leads to complete dissociation of Sirm from FYN. The binding of Sirm to FYN is intriguing, in view of the fact that FYN has been implicated in adipocyte-specific functions of insulin and particularly in the mechanism whereby insulin stimulates phosphorylation of caveolin in 3T3-L1 cells (25, 26). Caveolin is an important component of caveolae, flask-shaped invaginations of plasma membranes, which are thought to participate in the processing of intracellular signals. Some workers (27) have also reported that caveolae contain adapter molecules like Grb-2, which also binds to Sirm. It remains to be determined whether Sirm co-localizes with FYN in caveolae; however, it is interesting that a significant fraction of cellular Sirm is associated with the plasma membrane in 3T3-L1 adipocytes. Work from the Saltiel laboratory (26) has suggested that Cbl is the kinase responsible for stimulating the adipocyte-specific caveolin kinase activity of FYN. FYN kinase is activated by binding of cellular proteins to its SH2 and SH3 domains. Thus, an appealing possibility was that Sirm would regulate the FYN kinase in an adipocyte-specific fashion. We have failed to demonstrate that Sirm or peptides derived from it can modulate the kinase activity of FYN toward enolase. While these findings do not entirely rule out that Sirm may modulate the FYN kinase *in vivo*, they are consistent with data of Mastick *et al.* (26), suggesting that the kinase activity of FYN is not different in differentiated 3T3-L1

---

[3] Y. Kido, and D. Accili, manuscript in preparation.

cells compared with their undifferentiated counterpart. On the other hand, the identification of Sirm as an adipocyte-specific substrate of FYN raises the interesting possibility that Sirm may participate in adipocyte-specific functions of FYN.

The binding of Sirm to Grb-2 is also consistent with the known specificity of the Grb-2 SH3 binding domain (Fig. 2*B*) (28). The dissociation of Sirm from Grb-2 follows the same time course and dose responsiveness as insulin-induced dissociation of Grb-2 from son-of-sevenless (29, 30). This dissociation has been invoked as a possible mechanism underlying the transient nature of insulin's effect to activate Ras. By analogy, one could envision that Sirm links Grb-2 to downstream effectors and that this effect is lost upon prolonged insulin stimulation.

The evidence presented in this paper indicates that Sirm is a novel adapter protein, which can function in a variety of cell types by binding the Src family kinase FYN and Grb-2. Sirm expression appears to correlate with the ability of organs and cells to respond to insulin, and several of the intracellular targets of Sirm have been implicated in signaling downstream of the insulin receptor. We would like to tentatively propose that Sirm plays a role in modulating insulin action in insulin-sensitive tissues via its association with signaling molecules. Further studies required to conclusively test this hypothesis are under way.

REFERENCES

1. Joshi, R. L., Lamothe, B., Cordonnier, N., Mesbah, K., Monthioux, E., Jami, J., and Bucchini, D. (1996) *EMBO J.* **15,** 1542–1547
2. Accili, D., Drago, J., Lee, E. J., Johnson, M. D., Cool, M. H., Salvatore, P., Asico, L. D., Jose, P. A., Taylor, S. I., and Westphal, H. (1996) *Nat. Genet.* **12,** 106–109
3. Di Cola, G., Cool, M. H., and Accili, D. (1997) *J. Clin. Invest.* **99,** 2538–2544
4. Bruning, J. C., Winnay, J., Bonner, W. S., Taylor, S. I., Accili, D., and Kahn, C. R. (1997) *Cell* **88,** 561–572
5. Accili, D., and Taylor, S. I. (1991) *Proc. Natl. Acad. Sci. U. S. A.* **88,** 4708–4712
6. Frantz, J. D., Giorgetti-Peraldi, S., Ottinger, E. A., and Shoelson, S. E. (1997) *J. Biol. Chem.* **272,** 2659–2667
7. Kapeller, R., Prasad, K. V., Janssen, O., Hou, W., Schaffhausen, B. S., Rudd, C. E., and Cantley, L. C. (1994) *J. Biol. Chem.* **269,** 1927–1933
8. Reedquist, K. A., Fukazawa, T., Druker, B., Panchamoorthy, G., Shoelson, S. E., and Band, H. (1994) *Proc. Natl. Acad. Sci. U. S. A.* **91,** 4135–4139
9. Benian, G. M., Tinley, T. L., Tang, X., and Borodovsky, M. (1996) *J. Cell Biol.* **132,** 835–848
10. Wilson, R., Ainscough, R., Anderson, K., Baynes, C., Berks, M., Bonfield, J., Burton, J., Connell, M., Copsey, T., Cooper, J., Coulson, A., Craxton, M., Dear, S., Du, Z., Durbin, R., Favello, A., Fulton, L., Gardner, A., Green, P., Hawkins, T., Hillier, L., Jier, M., Johnston, L., Jones, M., Kershaw, J., Kirsten, J., Laister, N., Latreille, P., Lightning, J., Lloyd, C., McMurray, A., Mortimore, B., O'Callaghan, M., Parsons, J., Percy, C., Rifken, L., Roopra, A., Saunders, D., Shownkeen, R., Smaldon, N., Smith, A., Sonnhammer, E., Staden, R., Sulston, J., Thierry-Mieg, J., Thomas, K., Vaudin, M., Vaughan, K., Waterston, R., Watson, A., Weinstock, L., Wilkinson-Sproat, J., and Wohldman, P. (1994) *Nature* **368,** 32–38
11. Takeda, J., Yano, H., Eng, S., Zeng, Y., and Bell, G. I. (1993) *Hum. Mol. Genet.* **2,** 1793–1798
12. White, M. F., and Kahn, C. R. (1994) *J. Biol. Chem.* **269,** 1–4
13. Pawson, T. (1995) *Nature* **373,** 573–579
14. Rickles, R. J., Botfield, M. C., Weng, Z., Taylor, J. A., Green, O. M., Brugge, J. S., and Zoller, M. J. (1994) *EMBO J.* **13,** 5598–5604
15. Masters, J. N., Cotman, S. L., Osterburg, H. H., Nichols, N. R., and Finch, C. E. (1996) *Neuroendocrinology* **63,** 28–38
16. Ren, R., Mayer, B. J., Cicchetti, P., and Baltimore, D. (1993) *Science* **259,** 1157–1161
17. Parker, F., Maurier, F., Delumeau, I., Duchesne, M., Faucher, D., Debussche, L., Dugue, A., Schweighoffer, F., and Tocque, B. (1996) *Mol. Cell. Biol.* **16,** 2561–2569
18. Dai, Z., and Pendergast, A. M. (1995) *Genes Dev.* **9,** 2569–2582
19. Takeda, J., Espinosa, R. R., Eng, S., Le, B. M., and Bell, G. I. (1995) *Genomics* **29,** 276–281
20. Superti-Furga, G., Fumagalli, S., Koegl, M., Courtneidge, S. A., and Draetta, G. (1993) *EMBO J.* **12,** 2625–2634
21. Seidel-Dugan, C., Meyer, B. E., Thomas, S. M., and Brugge, J. S. (1992) *Mol. Cell. Biol.* **12,** 1835–1845
22. Zhu, J., and Shore, S. K. (1996) *Mol. Cell. Biol.* **16,** 7054–7062
23. Hanis, C. L., Boerwinkle, E., Chakraborty, R., Ellsworth, D. L., Concannon, P., Stirling, B., Morrison, V. A., Wapelhorst, B., Spielman, R. S., Gogolin, E. K., Shepard, J. M., Williams, S. R., Risch, N., Hinds, D., Iwasaki, N., Ogata, M., Omori, Y., Petzold, C., Rietzch, H., Schroder, H. E., Schulze, J., Cox, N. J., Menzel, S., Boriraj, V. V., Chen, X., Lim, L. R., Lindner, T., Mereu, L. E., Wang, Y.-Q., Xiang, K., Yamagata, K., Yang, Y., and Bell, G. I. (1996) *Nat. Genet.* **13,** 161–166
24. Weng, Z., Thomas, S. M., Rickles, R. J., Taylor, J. A., Brauer, A. W., Seidel, D. C., Michael, W. M., Dreyfuss, G., and Brugge, J. S. (1994) *Mol. Cell. Biol.* **14,** 4509–4521
25. Mastick, C. C., Brady, M. J., and Saltiel, A. R. (1995) *J. Cell Biol.* **129,** 1523–1531
26. Mastick, C. C., and Saltiel, A. (1997) *J. Biol. Chem.* **272,** 20706–20714
27. Wu, C., Butz, S., Ying, Y., and Anderson, R. G. W. (1997) *J. Biol. Chem.* **272,** 3554–3559
28. Sparks, A. B., Rider, J. E., Hoffman, N. G., Fowlkes, D. M., Quillam, L. A., and Kay, B. K. (1996) *Proc. Natl. Acad. Sci. U. S. A.* **93,** 1540–1544
29. Waters, S. B., Holt, K. H., Ross, S. E., Syu, L.-J., Guan, K.-L., Saltiel, A. R., Koretzky, G. A., and Pessin, J. E. (1995) *J. Biol. Chem.* **270,** 20883–20886
30. Waters, S. B., Yamauchi, K., and Pessin, J. E. (1995) *Mol. Cell. Biol.* **15,** 2791–2799